Accepted manuscript.

Final version published in:

J Am Soc Mass Spectrom. 2022 Jul 6;33(7):1176-1186.

doi: 10.1021/jasms.2c00031
https://pubs.acs.org/doi/10.1021/jasms.2c00031

Stepwise collision energy-resolved tandem mass spectrometric experiments for the improved identification of citrullinated peptides

*Arnold Steckel[1], Ágnes Révész[2], Dávid Papp[1,3], Katalin Uray[4], László Drahos[2], Gitta Schlosser[1]**

[1] MTA-ELTE Lendület Ion Mobility Mass Spectrometry Research Group, ELTE Eötvös Loránd University, Institute of Chemistry, Department of Analytical Chemistry, Pázmány Péter sétány 1/A, 1117 Budapest, Hungary

[2] Research Centre for Natural Sciences, MS Proteomics Research Group, Magyar tudósok körútja 2, 1117 Budapest, Hungary

[3] Hevesy György PhD School of Chemistry, ELTE Eötvös Loránd University, Pázmány Péter sétány 1/A, 1117 Budapest, Hungary

[4] MTA-ELTE Research Group of Peptide Chemistry, Eötvös Loránd Research Network (ELKH), ELTE Eötvös Loránd University, Pázmány Péter sétány 1/A, 1117 Budapest, Hungary

*E-mail address: gitta.schlosser@ttk.elte.hu

KEYWORDS: citrullination, posttranslational modifications (PTMs), collision-induced dissociation (CID), tandem mass spectrometry (MS/MS)

ABSTRACT

The use of tandem mass spectrometry (MS/MS) is a fundamental prerequisite of reliable protein identification and quantification in mass-spectrometry-based proteomics. In bottom-up and middle-down proteomics, proteins are identified by the characteristic fragments of their constituting peptides. Posttranslational modifications (PTMs) often further complicate proteome analyses. Citrullination is an increasingly studied PTM converting arginines to citrullines (Cit, X) and is implicated in several autoimmune and neurological diseases as well as different types of cancer. Confirmation of citrullination is known to be very challenging since it results in the same molecular mass change as Asn/Gln deamidation. In this study, we explore which MS/MS characteristics can be used for the reliable identification of citrullination. We synthesized several peptides incorporating Cit residues that model enzymatic cleavages of different proteins with verified or putative citrullination. Collision-induced dissociation (CID) was used to investigate the energy dependence of Byonic, Mascot scores and confirmed sequence coverage (CSC) alongside with the neutral loss of HNCO characteristic to citrulline side chains. We found that although the recommended values (19-45 V) for ramped collision energy settings cover the optimal Mascot, Byonic or %CSC scores effectively, the diagnostic HNCO loss from precursors and fragments may reach their maximum intensities at lower and higher collision energies, respectively. Therefore, we suggest broadening the ramp range to ~5-60V to get more favorable identification rates for citrullinated peptides. We also found that Byonic was more successful in correctly identifying citrullinated peptides with deamidated residues than Mascot.

INTRODUCTION

Protein citrullination or deimination is a posttranslational modification (PTM) converting arginines (Arg, R) to citrullines (Cit, X) [1]. The process is catalyzed by the protein arginine deiminase (PAD) enzyme family and requires the presence of Ca^{2+} ions [2]. Molecular mass of the modified proteins is increased by 0.9840 Da per modification which is the same for Asn and Gln deamidation [3]. The conversion also reduces the basicity of the species of interest altering their charge state distribution. Several proteins have been confirmed to be substrates of PADs including histones [4–7], filaggrin and keratin [8], myelin basic protein [9,10], glial fibrillary acidic protein [10], interleukin-8 [11,12] and ribosomal proteins [13]. Pathological conditions that are associated with an increased level of deimination [14] are – among others – rheumatoid arthritis [15], neurodegenerative diseases [16,17], and different types of cancer [18]. There is an increasing need for confident detection of citrullination in large-scale chromatography-coupled mass spectrometric experiments and some approaches have been demonstrated to be successful [19,20]. Mass spectrometric detection suffers from problems like the easy misinterpretation of deamidated peptides as citrullinated ones due to the shared mass increment of +0.9840 Da/*z* for modified peptides and inappropriate precursor selection [3]. However, this could be overcome by using the neutral loss of isocyanic acid (H-N=C=O) from citrulline residues as a diagnostic marker either from precursors or fragment ions. [21]. The loss of HNCO is specific to organic molecules containing an ureido group. Thus homocitrulline residues also display a loss of HNCO upon CID.

The extent of fragmentation and thus the quality of the spectra and the probability of a successful identification is highly dependent on the collision energy (CE) that is used; therefore, the selection of an optimal value or range is crucially important. A typical example of using an optimal value is exploited in Orbitraps using the normalized collision energy technology (NCE) while other instruments

took advantage of fragmenting throughout a CE range and merging the resulting spectra (rolling CE in Triple TOFs and CE ramping in QTOFs). Recently, CE effects for thousands of peptides were studied using QTOF and Orbitrap instruments. Based on this, more efficient protocols were provided for large scale proteomics studies that use optimum energies for Mascot score (identification score of database search characterizing the quality of MS/MS spectrum) and confirmed sequence coverage (CSC) [22,23]. For peptide identification, 28% NCE was found to be the optimal value on an Orbitrap mass spectrometer [24]. Confirmed sequence coverage of mAb peptides was also investigated and a workflow using a step of two collision energies 6-10 eV apart was suggested [22]. For posttranslationally modified peptides like *N*- or *O*-glycosylated ones, a stepped NCE value of 30% to 50% was found to be ideal by Cao et al. [25], but generally $(30 \pm 10)\%$ is used by the community [25–27]. For QTOF instruments equipped with a cyclic ion mobility cell commercialized by Waters the use of ramping CE in the 19-45 V regime for proteomics experiments is recommended.

The presence of certain amino acids may alleviate or hinder the generation of full fragment ion series from the precursors thus potentially increasing false positive/negative hits. An increased cleavage preference has been observed *N*-terminal to Pro residues in CID [28]. Our group also described an amino acid effect for citrulline residues in CID [29], and to a lesser extent in HCD [30], that results in a favorable cleavage *C*-terminal to these residues. This phenomenon was preserved in EThcD experiments as well for even Cit-containing peptides bearing other PTMs at the same time [31]. The citrulline effect was found not to be influenced considerably by the identity of the residue following or preceding Cit in our study involving more than 100 Cit-containing model peptides [30]. Besides the neutral loss of isocyanic acid and the Cit effect, another advantageous characteristic would have been the use of iminium ion of Cit [X] to further

confirm the presence of the modification. These iminium ions have been exploited during the deep proteomic profiling of 30 human tissues to validate citrullination sites [32], however, it was found that the false negative rate could be high.

From the commercially available proteomics search engines used for analyzing raw MS/MS data, Mascot scores and Byonic scores are two of the most popular ones. Byonic scores range from 0 to ~1000 for a peptide and describes the absolute quality of peptide-spectrum match (PSM), not the relative one compared to other peptide candidates. A PSM score should be considered good if it is above 300 and the identification is almost sure to be correct above 500 [33]. Mascot score is a probability-based score. The Mascot score of a given PSM depends solely on the quality of the match between the respective experimental and theoretical MS/MS spectrum and is independent of the size of protein sequence database.

To the best of our knowledge, only a few studies dealt with the CE dependence of scores generated by proteomics search engines and none of them discussed the HNCO loss in a CE dependent manner. The use of Byonic software and confirmed sequence coverage would also be beneficial for a more reliable identification of citrullination.

In this study, we used synthetic peptides containing Cit residues, mimicking enzymatic digestion of various human proteins that has previously been confirmed or suspected by similarity to be citrullinated. We aimed to investigate the Byonic and Mascot scores, the %CSC values and the HNCO losses from precursors and fragments in an energy-resolved way to find an optimum for the analysis of this PTM.

EXPERIMENTAL METHODS

Sequences of Cit-containing human peptides that have been synthesized for our experiments are summarized in **Table 1**.

Table 1 List of the human model peptides that were used for the experiments optimizing CID energies

Peptide Sequence	Observed charge state*	Protein	UniProt ID	References
^{252}DHGXGYFE^{259}	2+	heterogeneous nuclear ribonucleoprotein U	Q00839	13
^{261}FADLTDAAAXNAELLR^{276}	3+	glial fibrillary acidic protein	P14136	34
^{22}GAVLPXSAKE^{31}	2+	interleukin-8 (MDNCF-a)	P10145	12,35
^{31}IXIFDLGR^{38}	2+	60S ribosomal protein L10	P27635	13
^{363}TLPVVFDSPXNXGLK^{377}	3+	protein-arginine deiminase type-4	Q9UM07	36
^{22}VLXDNIQGITKPAIR^{36}	3+	histone H4	P62805	37
^{22}VPLSXTVR^{29}	2+	C-X-C motif chemokine 10	P02778	11
^{211}VXVFQATXGK^{220}	2+, 3+	protein-arginine deiminase type-4	Q9UM07	36
^{46}**XISGLIYEETR^{56}	2+, 3+	histone H4	P62805	37

Note that for ease of interpretation, the indexing follows the notation of the original (with the initiator methionine or signal peptide if applicable) and not the posttranslationally modified mature proteins. * Only charge states reaching a %rel intensity of >20% are depicted and were examined. ** Citrulline residues may occur at the *N*-termini of tryptic peptides as well [32]

Peptides were selected to model enzymatic cleavages with trypsin or Glu-C enzyme. The model peptides were synthesized on Wang-resin by solid-phase peptide chemistry using Fmoc/^{t}Bu strategy. The peptides cover a large range of sequence length with versatile amino acid composition. The set also includes peptides with two Cit residues. Additional peptides TLPVVFDSPRDXGLK (abbreviated as RDX) and TLPVVFDSPXDRGLK (abbreviated as XDR) originating from TLPVVFDSPXNXGLK (abbreviated as XNX) were also

synthesized to test the ability of the search engines to differentiate between isomer sequences containing both citrullination and Asn deamidation.

Purified peptides were dissolved in acetonitrile-water (1:1, *v*/*v*) containing 0.1% of formic acid and were diluted to a final concentration of 0.1 μM. These solutions were directly injected with a flow rate of 5.0 uL/min to the electrospray ion source of a Q-Orbitrap instrument (Q-Exactive Focus, Thermo Scientific, Bremen, Germany) in our preliminary experiments aiming to determine optimal collision energy values for maximum Mascot scores, %CSC, HNCO loss from precursors, Cit effect and [X] intensities. The spray voltage was 3.5 kV, the capillary temperature was 280 °C, the sheath and auxiliary gases were 5 and 3 arbitrary units, respectively. Tandem mass spectra were acquired for doubly protonated precursors with an isolation width of 2.0 m/z in the collision energy (CE) range of 10-60 eV with 2 eV steps. The resolution was set to 70 000 at *m*/*z* 200. The AGC target was set to the recommended $2*10^5$. The mass tolerance was determined according to the recommended protocol and was set to 5 ppm for precursors and 0.03 Da for fragment peaks. Optimal HCD CE ranges were determined as follows: %NCE values corresponding to the Mascot score values ≥13 (95% CI); %NCE values corresponding to CSC≥80%, HNCO values were considered ideal if being ≥5rel%, Cit effect was acknowledged if/where the *y* fragment corresponding to a Cit-Aaa cleavage was a sequential base peak and [X]≥1rel% values were accepted as optimal.

All further experiments were carried out on a QTOF instrument (Waters Select Series Cyclic IMS, Wilmslow, UK). The 0.1 uM peptide solutions were directly infused with a flow rate of 10 uL/min to the ion source. The capillary and cone voltages were set to 2.5 kV and 40 V, respectively. The source offset was 10 V. The source and desolvation temperature were 120 and 250 °C, respectively. The cone and the desolvation gases were set to 20 and 600 L/h. The nebulizer gas was set to 6 bar. Single stage MS data were acquired to

determine the charge state distribution of the peptides. Tandem mass spectra were acquired for doubly and triply charged precursors in the collision energy (CE) range of 0-100 V with 5 V steps in either the trap or the transfer collision cell of the instrument. While scanning the trap region, the transfer region was held at the default value of 4 V and while scanning the transfer, the trap region was held at the default value of 6 V. Measurements were carried out in W mode (resolution was 100 000 at 800 *m*/*z*).

Mascot scores of peptide spectrum matches were generated using the Mascot search engine (version v.2.5. Matrix Science, London, UK). Further, we employed Byonic v3.8.13 (Protein Metrics, Cupertino, CA). Due to the above-mentioned independence of protein database size of Mascot and Byonic scores, we performed the database search against one sequence: that of the investigated protein. Since in the present study we investigated synthetic model peptides with known sequence, the database search had no identification purposes. Rather, we used the identification score as a measure of the goodness of MS/MS spectrum from proteomics identification point of view. The Mascot score is not dependent on the size of protein database; therefore MS/MS spectra were searched against a single entry, the amino acid sequence of the corresponding protein (obtained from UniProt database). The enzyme was trypsin or Glu-C. Maximum 2 missed cleavages were allowed for almost all the model peptides. Exceptional case was the peptide SGXGKGGKGLGKGGAKR, where the number of missed cleavages was set to 5 taking into account the number of K/R amino acids in the sequence. The mass tolerance was determined according to the recommended protocol [38] and was set to 5 ppm for precursors and 0.01 Da for fragment peaks. Citrullination of arginine and deamidation of N and Q were selected as variable modifications. Byonic search parameters were set as follows: cleavage sites of K and R amino acids with C-terminal cleavage side for tryptic peptides and cleavage sites of D and E amino acids with C-terminal cleavage side for model peptides having enzymatic cleavage with Glu-C. Fully

specific digestion specificity was used in all cases. The number of missed cleavages was 2 in almost all cases; for the peptide sequence SGXGKGGKGLGKGGAKR it was increased to 5. Citrullination of arginine and N/Q deamidation was set as common modification, 5 and 10 ppm for parent and fragment mass tolerance, respectively. Several variables were collected from the Mascot output files (.dat) and Excel reports of Byonic search engine using the Serac program [22] in order to obtain energy dependent data. Several parameters were investigated as a function of CE including Byonic scores, Mascot scores, confirmed sequence coverage (%CSC), the neutral loss intensity of HNCO from precursors (HNCO prec) and the diversity of fragments showing a HNCO loss (HNCO fragm).

Statistical evaluation of the data was carried out using ROPstat. Comparisons were made using the Welch's modified t-test, and a *p*-value of <0.05 was accepted as significant.

RESULTS AND DISCUSSION

One of the most applied methods for protein identification is based on database search of MS/MS spectra resulting in peptide identifications. The confidence of peptide spectrum matches (PSMs) is typically characterized by a score value. In the present study, we aimed to find optimal CE for a set of citrullinated model peptides from proteomics identification point of view. For this purpose, we used the Byonic and Mascot score in this study.

The neutral loss of HNCO characteristic to citrulline residues, are long-time known and applied in the screening of citrullinated peptides/proteins. In addition, confirmed sequence coverage (%CSC), a recent technique developed for better identification of proteins, may be advantageous for the confirmation of citrullination as well.

In this study, we investigated all these characteristics as dependent variables of CID collision energies. To the best of our knowledge, the CE dependence of confirmed sequence coverage for citrullinated peptides or HNCO loss from citrullinated peptides has not been investigated before. Synthetic isomer model peptides containing both citrullinated or deamidated residues has also not been investigated before in such details by scoring engines.

First, we used a Q-Orbitrap instrument for preliminary experiments. Mascot scores, %CSC values, HNCO loss intensity from precursors, the Cit effect and Cit iminium ion ([X]) intensities were examined as a function of CE values (**Table S1**). These data suggested that the use of a ~10-20% normalized collision energy results in fair Mascot and %CSC scores, while higher energies may be better for emphasizing Cit effect and [X] intensities (**Figure S1**). However, the latter two could often be unreliable and/or insufficient for exact Cit site determination (**Figure S2)**, therefore these variables were left out in the following.

All further experiments were carried out on a QTOF instrument. Beside Mascot scores we also examined Byonic scores. Moreover, HNCO losses were investigated for fragments too, not only for precursor ions. The best scores (Byonic, Mascot) and maximal values for precursor HNCO loss (HNCO prec) and maximal number of HNCO losses from fragments (HNCO fragm) are listed in **Table 2.** Detailed data and breakdown curves could be found in **Table S2-S6** and **Figures S3-S7** respectively.

Table 2 Best scores and maximal values of the examined variables for the nine model peptides. Only true positive matches are listed here. For false positive matches, see **Table S7**.

Sequence	Charge state	Type	Best Byonic	Best Mascot	Best %CSC	HNCO prec[1]	2 HNCO prec[2]	HNCO fragm[3]
DHGXGYFE	2	Transfer	439.8	37.80	100	16%	-	4
GAVLPXSAKE	2	Transfer	794.8	50.76	100	8%	-	5
IXIFDLGR	2	Transfer	528.7	40.32	100	6%	-	2
VPLSXTVR	2	Transfer	462.2	55.57	100	18%	-	9
VXVFQATXGK	2	Transfer	623.9	74.50	100	31%	4.3%	8
XISGLIYEETR	2	Transfer	661.6	82.16	100	5%	-	0
DHGXGYFE	2	Trap	461.0	36.39	100	21%	-	4
GAVLPXSAKE	2	Trap	765.3	52.71	100	8%	-	6
IXIFDLGR	2	Trap	511.0	45.27	100	6%	-	2
VPLSXTVR	2	Trap	434.7	72.79	100	11%	-	7
VXVFQATXGK	2	Trap	616.4	70.76	100	38%	5.2%	7
XISGLIYEETR	2	Trap	652.9	87.72	100	6%	-	1
FADLTDAAAXNAELLR	3	Transfer	888.1	82.02	100	15%	-	8
TLPVVFDSPXNXGLK	3	Transfer	777.2	74.41	100	2%	0.01%	7
VLXDNIQGITKPAIR	3	Transfer	694.7	82.34	86.67	24%	-	2
VXVFQATXGK	3	Transfer	657.6	42.31	100	7%	0.7%	8
XISGLIYEETR	3	Transfer	583.7	78.33	100	0%	-	2
FADLTDAAAXNAELLR	3	Trap	873.3	76.48	100	16%	-	8
TLPVVFDSPXNXGLK	3	Trap	747.5	49.55	86.67	2%	0.0%	7
VLXDNIQGITKPAIR	3	Trap	718.4	87.97	100	31%	-	2
VXVFQATXGK	3	Trap	658.2	36.13	100	9%	1.0%	8
XISGLIYEETR	3	Trap	599.8	78.96	81.82	0%	-	1

[1] neutral loss of isocyanic acid (HNCO) given in relative base peak percentage
[2] neutral loss of 2 molecules of HNCO given in relative base peak percentage
[3] number of neutral loss of HNCO from fragment ions (b, y)

We compared the variable values of doubly and triply protonated precursors. Interestingly there were no significant differences (Table S8) despite of the observation that a higher charge state precursor is generally easier to be activated by collisions due to the repulsion of alike charges. This means that an easier activation does not necessarily yield more diverse fragment ion series.

We also compared the results for the two collision cells available in the QTOF instrument. It can be concluded that there were no significant differences between them either at a confidence level of 95% (Table S9).

The CE dependence data corresponding to maximum values of the variables were also plotted and were categorized by fragmentation type (transfer or trap) and precursor charge state in **Figure 1**.

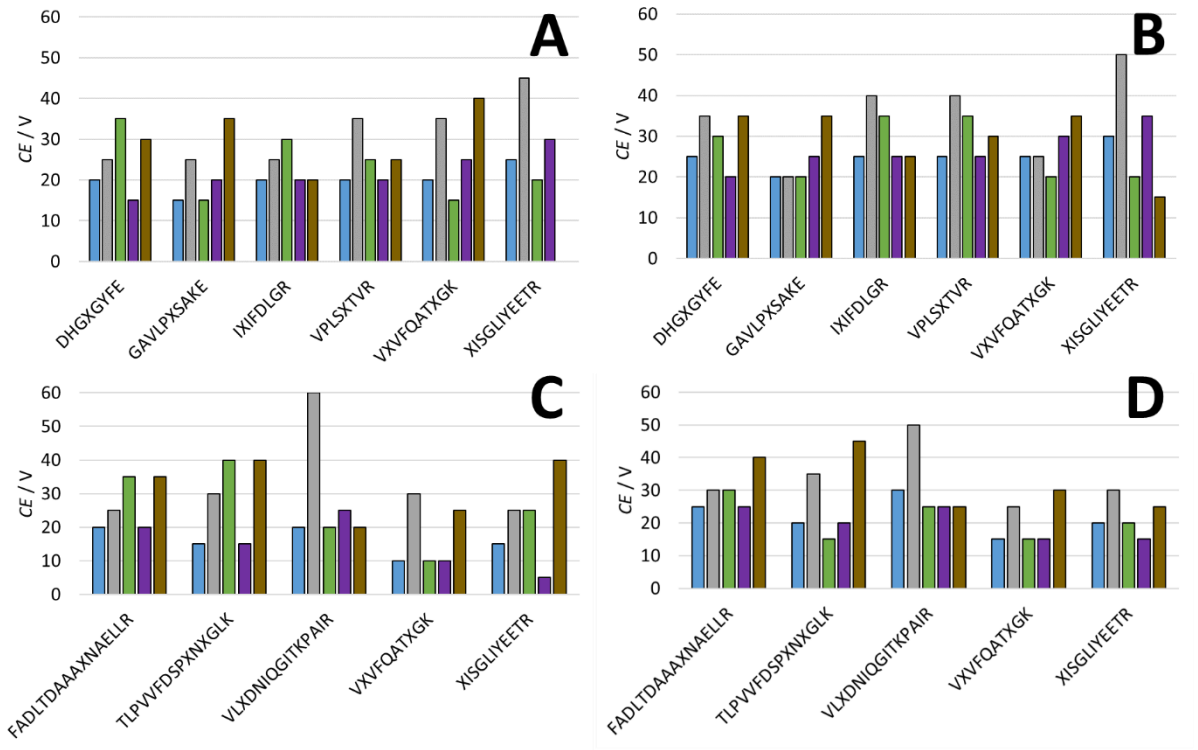

Figure 1 Collision energies corresponding to maximal Byonic scores (blue), Mascot scores (gray), %CSC scores (green), HNCO prec (purple) and HNCO fragm (brown) for doubly protonated precursors in the transfer and the trap (A and B, respectively) and triply protonated precursors in the transfer and trap (C and D, respectively). Only a single loss of HNCO from precursors is shown.

Note that theoretically a double loss of HNCO is expected from precursors containing two Cit residues, however, a second loss of HNCO was only detected for VXVFQATXGK 2+ in an appreciable amount (see also **Table 2**). This indicates that the reliable identification of multiply citrullinated peptides may be even more difficult.

To better visualize these data, CE value ranges covering the maximal Byonic scores, Mascot scores, %CSC, and the loss of HNCO from precursors and fragments are shown for all peptides in **Figure 2** as a box and whisker plot.

CE range corresponding to maximum Mascot scores (gray box) for doubly protonated precursors in the transfer collision cell is higher than that of Byonic scores (blue box) and HNCO prec scores (purple box) (**Figure 2A**). CE values corresponding to HNCO fragm (brown box) values are slightly higher than that of HNCO prec and Byonic scores. For triply protonated precursors fragmented in the transfer collision cell, similar, but more pronounced differences are measured (**Figure 2C**). The optimal range is, however, a bit more variable.

Data obtained by fragmentation of doubly protonated precursors in the trap cell (**Figure 2B**) are similar to that of the transfer cell. However, CE values corresponding to Mascot scores are slightly higher than that of Byonic scores and not higher than HNCO prec. CE values corresponding to HNCO fragm values are not higher than that of HNCO prec or Byonic either. For triply protonated trap fragmentation data (Figure 2D), CE values corresponding to Mascot scores are higher than that of Byonic scores, HNCO prec values (and also that of %CSC values very slightly), while CE values corresponding to HNCO fragm values are also higher than that of HNCO prec and Byonic scores.

The determined optimal CE settings are lower for Byonic than for Mascot search engine. An in-depth analysis of this difference would require the knowledge and comparison of the scoring algorithms of the search engines. Since Byonic is a commercial software, we refrain from a detailed explanation of this phenomena. On the other hand, similar trend was found for unmodified tryptic peptides [24] earlier. The key reasons may include the difference in what types of fragment ions the engines look for and how they utilize experimental intensity information. The investigation of tryptic peptides already indicated that Byonic considers more of the low intensity *b* fragment ions that favor low energies resulting in lower optimal CE. The Byonic's higher focus on less intense fragment ions may also contribute to the better capability of correctly identifying the deamidation position (see below).

Comparing the transfer and trap collision cell fragmentation data, the optimal CE corresponding to Byonic scores obtained in the trap was significantly higher ($p=0.02$) in the group of doubly protonated precursors than that of the transfer collision cell but only slightly significantly higher ($p=0.10$) in the group of triply protonated precursors (Table S10). Other data were not significantly different between the two groups.

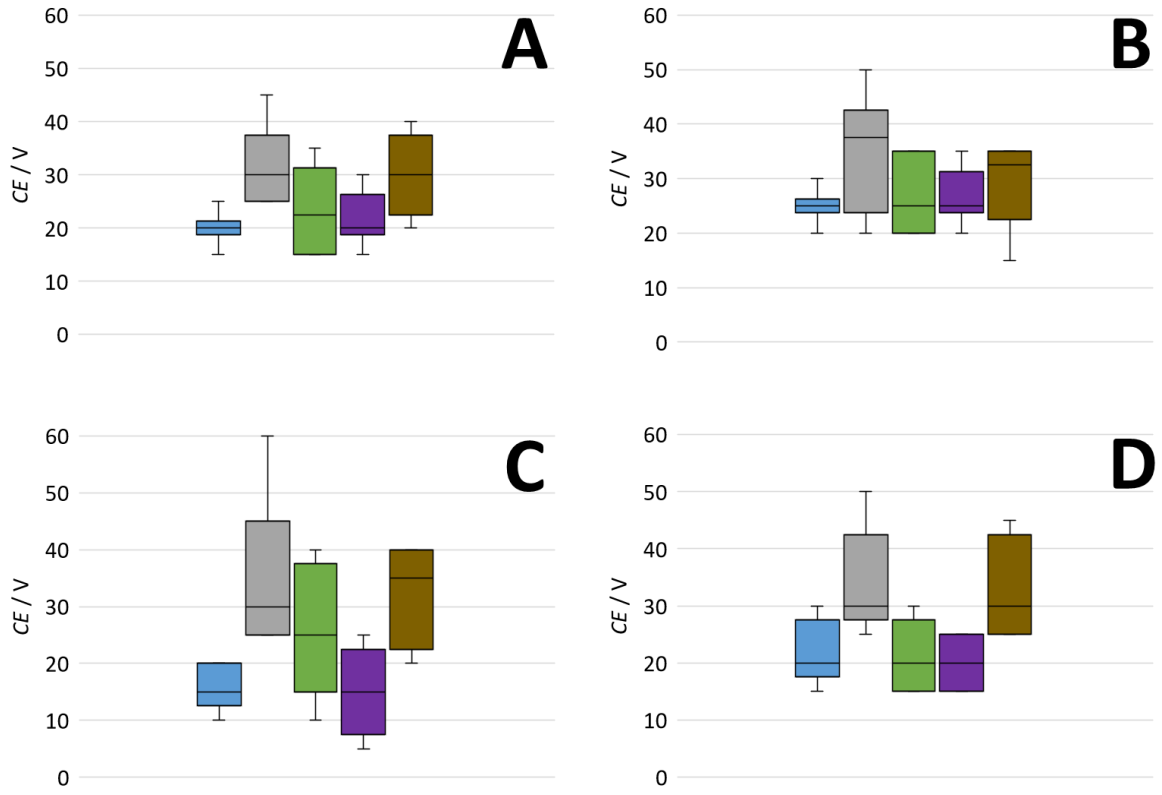

Figure 2 CE ranges corresponding to the maximal values of the six variables that were investigated for doubly protonated precursors in the transfer (A) and the trap (B) and triply protonated precursors in the transfer (C) and trap (D). Byonic scores (blue), Mascot scores (gray), %CSC scores (green), HNCO prec (purple) and HNCO fragm (brown) are depicted with a box and whisker plot.

To illustrate differences in MS/MS fragmentation patterns at CE values corresponding to best scores and variable values, the fragmentation of the triply protonated FADLTDAAAXNAELLR peptide is shown in **Figure 3**. It could be seen that choosing a 20-25 V is optimal for Byonic, Mascot score and HNCO prec (**Figure 3A, B**) but not optimal for %CSC and HNCO fragm (**Figure B, C**). Curves of HNCO losses from precursors as a function of CE also tend to be broken down very quickly. Note the abundant y_6 ion in the spectra that is caused by the so-called 'citrulline effect', an enhanced cleavage *C*-terminal to citrulline residues. [30,39] Cit effect was also observed for IXIFDLGR, VXVFQATXGK (2+) and to a lesser extent,

VLXDNIQGITKPAIR peptides. The full series of ***y*** ions showing HNCO losses presented here is unfortunately not a characteristic feature to all peptide precursors. For example, XISGLIYEETR only showed maximum one or two HNCO losses or no HNCO loss from fragments depending on precursor charge state and the location of fragmentation (transfer or trap collision cell) (**Table 2**).

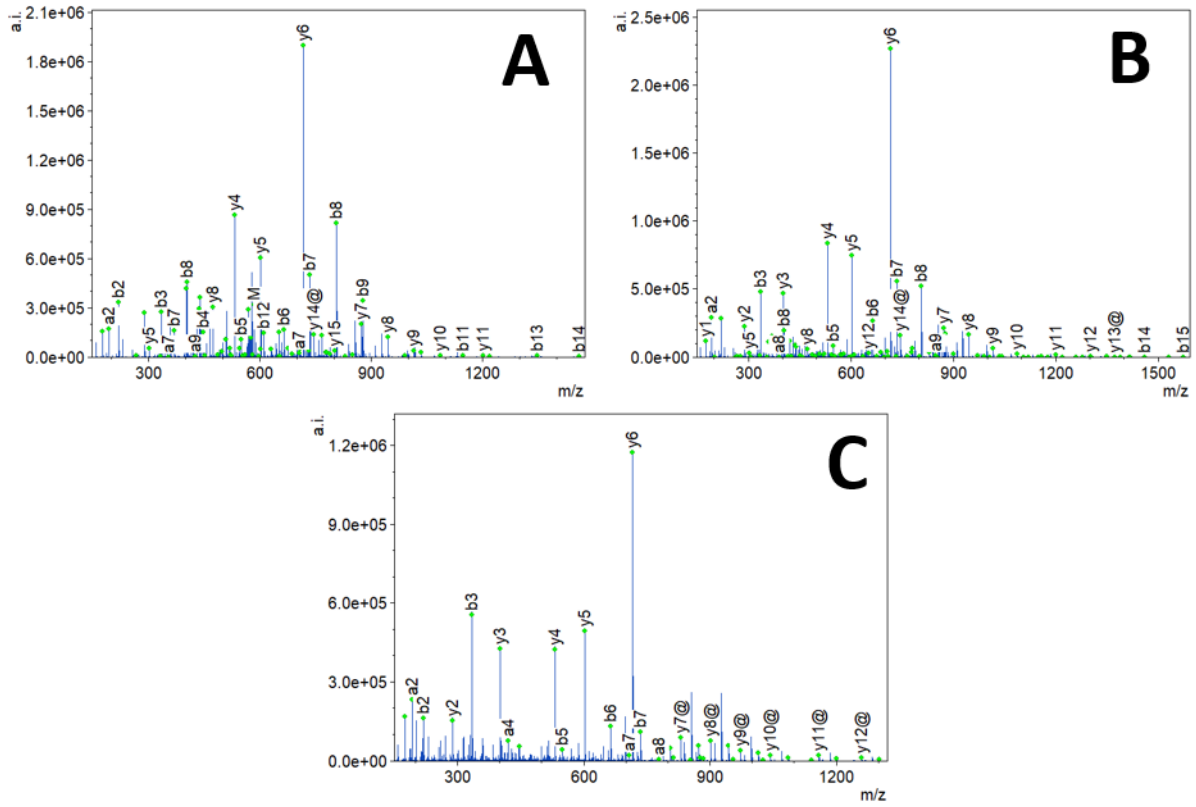

Figure 3 CID MS/MS spectra of triply protonated FADLTDAAAXNAELLR peptide in the transfer collision cell corresponding to optimal Byonic score and HNCO prec at 20 V (A), Mascot score at 25 V (B), %CSC and the highest diversity of fragment HNCO losses at 35V (C). Isocyanic acid loss is depicted as @.

Doubly protonated VPLSXTVR is another example for attaining a full sequence coverage and HNCO-loss detection from all possible fragments having a citrulline residue in them at the same time (**Figure 4**). Also note the highly abundant y_7 (2+) ion caused by the 'proline effect' that is an enhanced cleavage preference *N*-terminal to Pro residues.

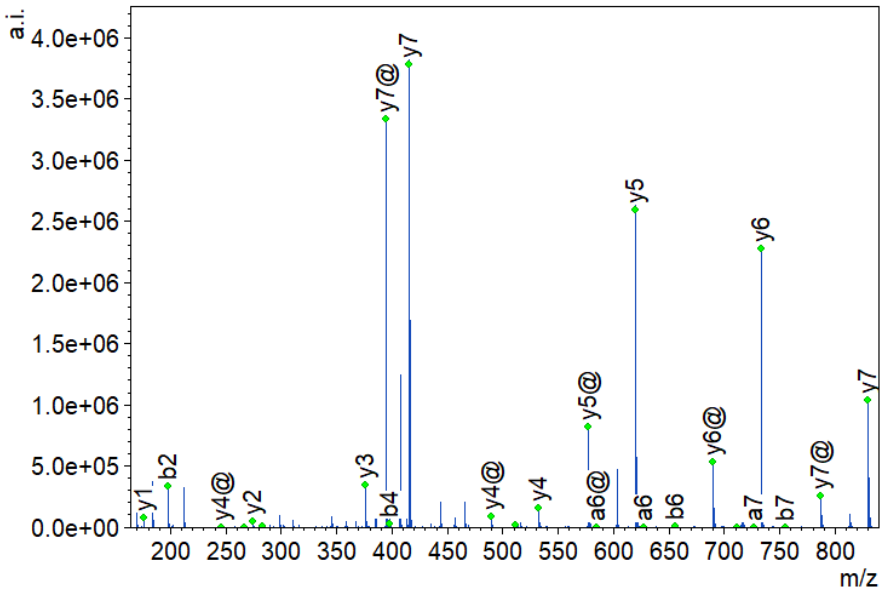

Figure 4 CID MS/MS spectra of doubly protonated VPLSXTVR in the transfer collision cell (25V) as an illustration of an ideal citrullinated peptide spectrum. The precursor and all fragments containing a Cit residue display an abundant HNCO loss unambiguously verifying the position of the modification. Full sequence coverage of ***y*** ions criterion is also fulfilled.

Setting deamidation of N/Q besides citrullination introduced a number of false positive matches for our model peptides (Table S7). This number, however, was much less for Byonic search engine which was generally able to selectively and reliably identify the true positive matches in a broad range of collision voltage (Figure 5, Figures S8-S10).

Mascot found several candidates, but in all cases, the true positive match got the highest score in a broad range of collision voltage (Figure 5).

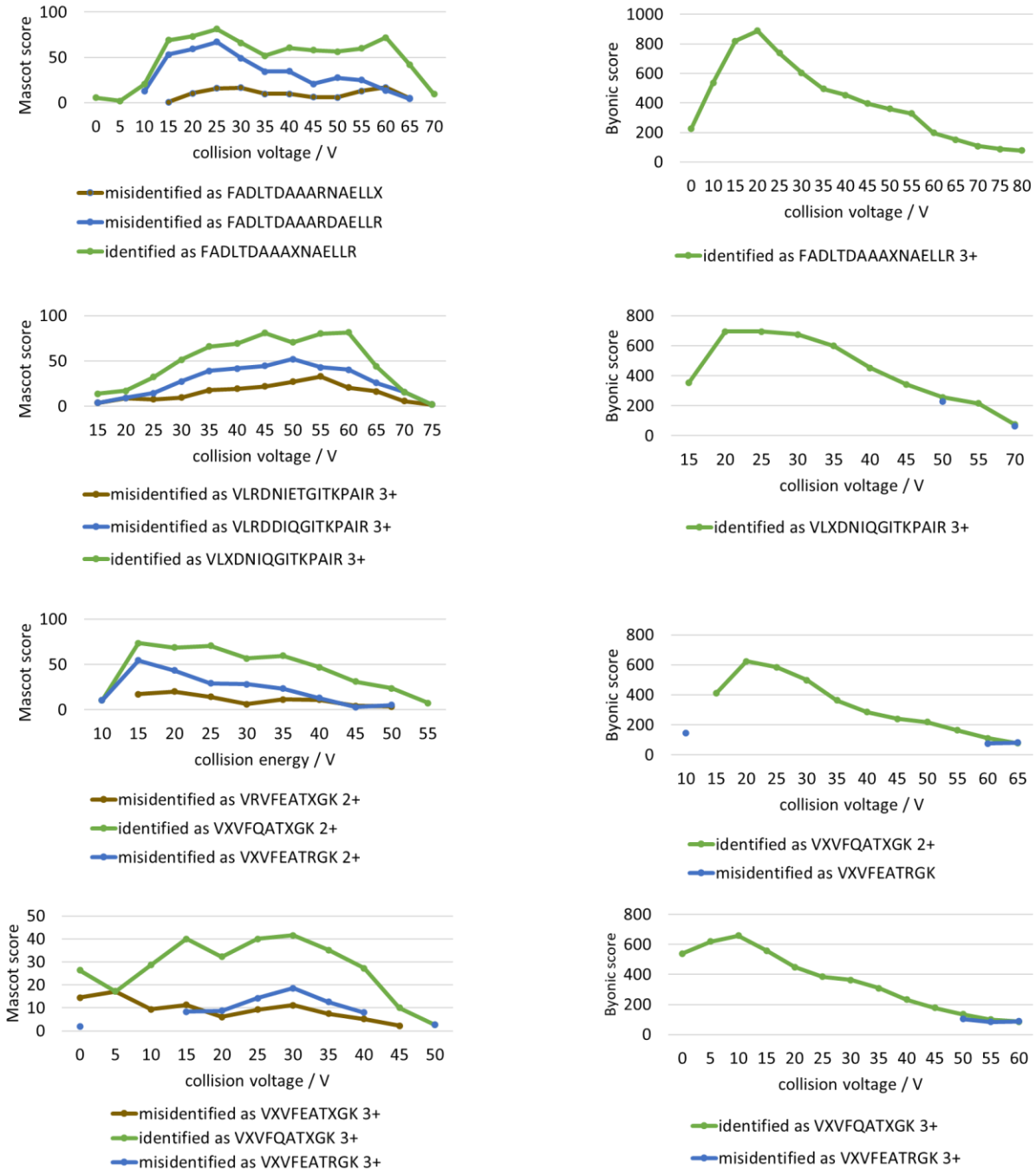

Figure 5 CE dependence of Mascot (left panel) and Byonic (right): panel of the nine model peptides when deamidation is also set as a variable modification during search. Only sequences with an N/Q residue are shown.

We also performed energy-dependent experiments on the isomer sequences TLPVVFDSPRDXGLK (RDX) and TLPVVFDSPXDRGLK (XDR) of the original sequence TLPVVFDSPXNXGLK (XNX) to test whether Byonic and Mascot search engines can differentiate between the three (Figure 6).

Figure 6 Energy dependence of Mascot and Byonic scores for triply protonated TLPVVFDSPRDXGLK (upper), TLPVVFDSPXDRGLK (middle) and TLPVVFDSPXNXGLK (bottom) in the transfer collision cell.

Our results show that Mascot search engine usually identifies the true isomer albeit along with the other two possible false isomers. The scores of the true and false isomers are usually too close to each other to reliably identify the true isomer, but in the case of the XDR peptide, Mascot successfully differentiates the true isomer from RDX and XNX in the 25-35V and 40-60 collision coltage range. On the other hand, Byonic search engine was somewhat more selective than Mascot. Moreover, in the case of XDR sequence, Byonic identified correctly the true isomer in almost the whole collision voltage range. Byonic could also identify the true isomer in the case of XNX in the standard collision energy range of ~20-45 V, while Mascot misidentified it as XDR (Figure 6, bottom panel). This is a good case study when search engines fail to reliably identify a peptide sequence even under well-controlled circumstances.

As our results suggested that the use of a 19-45 V ramped collision energy recommended by the manufacturer may not always cover the whole ranges corresponding to best scores, we performed measurements of 5-60 V ramped collision energy and compared our results with that of 19-45 V for all the model peptides that have been investigated by the previous energy-dependent manner. Our results show that the two datasets do not differ statistically (Table 3). Precursor HNCO loss intensities were generally lower in the 5-60 V range, however, these values are sufficient for a reliable detection. Moreover, in several cases, where the %rel intensity was 0% in 19-45 V, considerable improvement can be seen in the 5-60 V range (TLPVVFDSPXNXGLK, VXVFQATXGK, TLPVVFDSPXDRGLK). On the other hand, %CSC values improved in two cases (GAVLPXSAKE and TLPVVFDSPXNXGLK), while all other %CSC values remained the same 100%. Statistics in this case could not indicate significance but this may be because 100% is the upper limit of sequence coverage.

Table 3 Results of ramped collision energy experiments in the transfer collision cell for our model peptides. Only true matches are shown in the table. False matches are listed in Table S11.

Sequence	Charge	Byonic		Mascot		%CSC		HNCO prec (%)		HNCO fragm (#)	
		19-45 V	5-60 V	19-45 V	5-60 V	19-45 V	5-60 V	19-45 V	5-60 V	19-45 V	5-60 V
DHGXGYFE	2	480.3	558.6	43.81	35.94	100	100	9.6	6.7	4	1
FADLTDAAAXNAELLR	3	822.0	798.7	74.92	72.26	100	100	3.3	1.7	1	1
GAVLPXSAKE	2	606.9	668.8	48.37	53.64	60	80	4.2	3.7	1	1
IXIFDLGR	2	464.3	476.7	52.86	43.23	100	100	1.9	2.7	0	0
TLPVVFDSPXNXGLK	3	554.7	616.5	59.14	44.36	73.33	86.67	0.0	1.1	0	8
VLXDNIQGITKPAIR	3	706.0	631.2	49.35	36.11	100	100	46.7	5.1	0	1
VPLSXTVR	2	388.1	404.4	53.80	50.33	100	100	12.1	6.7	5	4
VXVFQATXGK	2	579.4	548.6	56.44	54.24	100	100	31.9	4.8	5	2
VXVFQATXGK	3	415.8	640.8	37.61	32.97	100	100	0.0	11.1	8	3
XISGLIYEETR	2	642.3	577.5	55.51	66.32	100	100	4.7	1.0	1	0
XISGLIYEETR	3	520.0	621.3	57.21	56.53	100	100	0.0	0.0	0	0
TLPVVFDSPRDXGLK	3	426	443.6	39.09	36.90	80	73.33	0.0	0.1	9	6
TLPVVFDSPRDXGLK	4	433.8	457.7	3.80	10.03	60	60	0.0	0.5	2	1
TLPVVFDSPXDRGLK	3	634.9	657.3	44.63	30.08	73.33	73.33	0.0	0.8	5	1
TLPVVFDSPXDRGLK	4	400.9	351.7	-	-	-	-	0.0	1.3	-	-
p-value		0.58		0.53		0.74		0.23		0.42	

CONCLUSIONS

In conclusion, we recommend the use of ramped collision energy of ~5-60 V for MS/MS of doubly-triply charged middle-sized (~8-15 constituting amino acids) citrullinated peptides to reliably detect the diagnostic loss of HNCO from precursors and fragments as well, and to obtain an ideal sequential coverage (%CSC), Byonic score and Mascot score at the same time. This range is slightly broader than that of the recommendation of the manufacturer (19-45 V) due to our observation that HNCO losses from precursors tend to occur at lower CE values while the diversity of HNCO losses from fragment ions tend to be optimal at higher CE values. A CE ramp of ~20-40V is however usually acceptable to reach a good sequence coverage and to detect some

fragments showing a HNCO loss verifying the presence of citrullination. We did not find significant differences between MS/MS spectra acquired in the trap and transfer collision cells so they could be used interchangeably depending on the task without remarkable compromising of the identification scores or other variables.

We also found that CE values corresponding to Mascot scores were significantly higher than that of Byonic ones. Byonic search engine was found to be more selective in identification of citrullination, generally finding only the true positive matches in cases when deamidation of N/Q and citrullinated residues were also present and they were set as variable modifications. Mascot search engine usually found all possible differentially modified sequences – including false positive matches – but generally gave them lower identification scores. To the best of our knowledge no other studies have investigated the collision energy-dependence of identification scores for model peptides containing citrullines in details like this.

ASSOCIATED CONTENT

Supplementary File 1

Table S1 Detailed data of the model peptides and their determined optimal values for the preliminary Orbitrap experiments. Optimal values are expressed in the corresponding %NCE.

Table S2 The collision energy dependence of Byonic scores based on the QTOF experiments

Table S3 The collision energy dependence of Mascot scores based on the QTOF experiments

Table S4 The collision energy dependence of %CSC values based on the QTOF experiments

Table S5 The collision energy dependence of HNCO prec values based on the QTOF experiments

Table S6 The collision energy dependence of HNCO fragm values based on the QTOF experiments

Table S7 Best Byonic and Mascot scores for the false positive matches of the nine model peptides

Table S8 Statistical comparison of doubly and triply protonated precursor data (dependent variables) for the transfer and trap collision cell. Results are given by the *p*-value of the Welch's modified t-test.

Table S9 Statistical comparison of transfer and trap collision cell data for doubly and triply protonated precursors. Results are given by the *p*-value of the Welch's modified t-test.

Table S10 Statistical comparison of transfer and trap collision cell data for doubly and triply protonated precursors corresponding to the optimal CE values. Results are given by the *p*-value of the Welch's modified t-test

Table S11 False match results from the ramped collision energy experiments. The first line for example corresponding to FADLTDAAARDAELLR is a false match for the sample FADLTDAAAXNAELLR; VXVFEATRGK is a false match for the sample containing only VXVFQATXGK. In the case of the lower lines, 'from XDR' means that this false sequence comes from the peptide TLPVVFDSPXDRGLK

Figure S1 The %NCE corresponding to the maximal Mascot scores, %CSC, the loss of HNCO from precursors and [X] intensities for the ten model peptides investigated by the Q-Orbitrap instrument.

Figure S2 Optimal normalized collision energy values for the ten model peptides investigated by the Q-Orbitrap instrument. Optimal median Mascot scores (A), median %CSC (B), median range for loss of HNCO (C), median range for Cit effect (D) and median range for [X] intensities (E).

Figure S3 Graphical representation of the collision energy dependence of Byonic scores for the model peptides

Figure S4 Graphical representation of the collision energy dependence of Mascot scores for the model peptides

Figure S5 Graphical representation of the collision energy dependence of %CSC scores for the model peptides

Figure S6 Graphical representation of the collision energy dependence of HNCO prec values for the model peptides

Figure S7 Graphical representation of the collision energy dependence of HNCO fragm values for the model peptides

Figure S8 The CE dependence of Mascot (left panel) and Byonic scores (right panel) for triply protonated VLXDNIQGITKPAIR in the transfer cell

Figure S9 The CE dependence of Mascot (left panel) and Byonic scores (right panel) for doubly protonated VXVFQATXGK in the transfer cell

Figure S10 The CE dependence of Mascot (left panel) and Byonic scores (right panel) for triply protonated VXVFQATXGK in the transfer cell

AUTHOR INFORMATION

Corresponding Author

*Gitta Schlosser

E-mail address: gitta.schlosser@ttk.elte.hu

Author Contributions

The manuscript was written through contributions of all authors. All authors have given approval to the final version of the manuscript.

ACKNOWLEDGMENT

This project was supported by the Lendület (Momentum) Program of the Hungarian Academy of Sciences (HAS, MTA). This work was completed in the ELTE Thematic Excellence Programme supported by the Hungarian Ministry for Innovation and Technology. The research within Project No. VEKOP-2.3.3-15-2017-00020 were supported by the European Union and the State of Hungary, cofinanced by the European Regional Development Fund. Project No. 2018-1.2.1-NKP-2018-00005 has been implemented with the support provided from the National Research, Development and Innovation Fund of Hungary, financed under the 2018-1.2.1-NKP funding scheme. Á.R. was supported by the János Bolyai Research Scholarship of the Hungarian Academy of Sciences. Funding from the National Research, Development and Innovation Office (NKFIH PD-132135 and K 131762) is gratefully acknowledged.

ABBREVIATIONS

CL, confidence level; CID, collision-induced dissociation; Cit, three-letter abbreviation for citrulline; %CSC, confirmed sequence coverage; EThcD, electron transfer higher energy collision(al) dissociation; HCD, higher-energy collisional dissociation; MS/MS, tandem mass spectrometry; %NCE, normalized collision energy; PAD, protein arginine deiminase; PSM, peptide spectrum match, PTM, posttranslational modification; X, one-letter abbreviation for citrulline.

REFERENCES

(1) Nicholas, A. P.; Thompson, P. R.; Bhattacharya, S. K. *Protein Deimination in Human Health and Disease*; 2017. https://doi.org/10.1007/978-3-319-58244-3.

(2) Tilvawala, R.; Thompson, P. R. Peptidyl Arginine Deiminases: Detection and Functional Analysis of Protein Citrullination. *Curr. Opin. Struct. Biol.* **2019**, *59*, 205–215. https://doi.org/10.1016/j.sbi.2019.01.024.

(3) Verheul, M. K.; van Veelen, P. A.; van Delft, M. A. M.; de Ru, A.; Janssen, G. M. C.; Rispens, T.; Toes, R. E. M.; Trouw, L. A. Pitfalls in the Detection of Citrullination and Carbamylation. *Autoimmun. Rev.* **2018**, *17* (2), 136–141. https://doi.org/10.1016/j.autrev.2017.11.017.

(4) Wang, Y.; Wysocka, J.; Sayegh, J.; Lee, Y. H.; Pertin, J. R.; Leonelli, L.; Sonbuchner, L. S.; McDonald, C. H.; Cook, R. G.; Dou, Y.; Roeder, R. G.; Clarke, S.; Stallcup, M. R.; Allis, C. D.; Coonrod, S. A. Human PAD4 Regulates Histone Arginine Methylation Levels via Demethylimination. *Science* **2004**, *306* (5694), 279–283. https://doi.org/10.1126/science.1101400.

(5) Hagiwara, T.; Hidaka, Y.; Yamada, M. Deimination of Histone H2A and H4 at Arginine 3 in HL-60 Granulocytes. *Biochemistry* **2005**, *44* (15), 5827–5834. https://doi.org/10.1021/bi047505c.

(6) Miao, F.; Li, S. L.; Chavez, V.; Lanting, L.; Natarajan, R. Coactivator-Associated Arginine Methyltransferase-1 Enhances Nuclear Factor-Kb-Mediated Gene Transcription through Methylation of Histone H3 at Arginine 17. *Mol. Endocrinol.* **2006**, *20* (7), 1562–1573. https://doi.org/10.1210/me.2005-0365.

(7) Arita, K.; Shimizu, T.; Hashimoto, H.; Hidaka, Y.; Yamada, M.; Sato, M. Structural Basis for Histone N-Terminal Recognition by Human Peptidylarginine Deiminase 4. *Proc. Natl. Acad. Sci. U. S. A.* **2006**, *103* (14), 5291–5296. https://doi.org/10.1073/pnas.0509639103.

(8) Senshu, T.; Kan, S.; Ogawa, H.; Manabe, M.; Asaga, H. Preferential Deimination of Keratin K1 and Filaggrin during the Terminal Differentiation of Human Epidermis The Process of Normal Epidermal Differentiation Is Characterized by a Series of Morphologic Changes as Keratinocytes Progress from the Germinative . *Biochem. Biophys. Res. Commun.* **1996**, *719*, 712–719.

(9) Wood, D. D.; Moscarello, M. A. The Isolation, Characterization, and Lipid-Aggregating Properties of a Citrulline Containing Myelin Basic Protein. *J. Biol. Chem.* **1989**, *264* (9), 5121–5127.

(10) Jin, Z.; Fu, Z.; Yang, J.; Troncosco, J.; Everett, A. D.; Van Eyk, J. E. Identification and Characterization of Citrulline-Modified Brain Proteins by Combining HCD and CID Fragmentation. *Proteomics* **2013**, *13* (17), 2682–2691. https://doi.org/10.1002/pmic.201300064.

(11) Loos, T.; Mortier, A.; Gouwy, M.; Ronsse, I.; Put, W.; Lenaerts, J. P.; Van Damme, J.; Proost, P. Citrullination of CXCL10 and CXCL11 by Peptidylarginine Deiminase: A Naturally Occurring Posttranslational Modification of Chemokines and New Dimension of Immunoregulation. *Blood* **2008**, *112* (7), 2648–2656. https://doi.org/10.1182/blood-2008-04-149039.

(12) Proost, P.; Loos, T.; Mortier, A.; Schutyser, E.; Gouwy, M.; Noppen, S.; Dillen, C.; Ronsse, I.; Conings, R.; Struyf, S.; Opdenakker, G.; Maudgal, P. C.; Van Damme, J. Citrullination of CXCL8 by Peptidylarginine Deiminase Alters Receptor Usage, Prevents Proteolysis, and Dampens Tissue Inflammation. *J. Exp. Med.* **2008**, *205* (9), 2085–2097. https://doi.org/10.1084/jem.20080305.

(13) Christophorou, M. A.; Castelo-Branco, G.; Halley-Stott, R. P.; Oliveira, C. S.; Loos, R.; Radzisheuskaya, A.; Mowen, K. A.; Bertone, P.; Silva, J. C. R.; Zernicka-Goetz, M.; Nielsen, M. L.; Gurdon, J. B.; Kouzarides, T. Citrullination Regulates Pluripotency and Histone H1 Binding to Chromatin. *Nature* **2014**, *507* (7490), 104–108. https://doi.org/10.1038/nature12942.

(14) Vitorino, R.; Guedes, S.; Vitorino, C.; Ferreira, R.; Amado, F.; Van Eyk, J. E. Elucidating Citrullination by Mass Spectrometry and Its Role in Disease Pathogenesis. *J. Proteome Res.* **2021**, *20* (1), 38–48. https://doi.org/10.1021/acs.jproteome.0c00474.

(15) Darrah, E.; Andrade, F. Rheumatoid Arthritis and Citrullination. *Curr. Opin. Rheumatol.* **2018**, *30* (1), 72–78. https://doi.org/10.1097/BOR.0000000000000452.

(16) Faigle, W.; Cruciani, C.; Wolski, W.; Roschitzki, B.; Puthenparampil, M.; Tomas-Ojer, P.; Sellés-Moreno, C.; Zeis, T.; Jelcic, I.; Schaeren-Wiemers, N.; Sospedra, M.; Martin, R.

Brain Citrullination Patterns and T Cell Reactivity of Cerebrospinal Fluid-Derived CD4+ T Cells in Multiple Sclerosis. *Front. Immunol.* **2019**, *10* (APR), 1–17. https://doi.org/10.3389/fimmu.2019.00540.

(17) Gallart-Palau, X.; Tan, L. M.; Serra, A.; Gao, Y.; Ho, H. H.; Richards, A. M.; Kandiah, N.; Chen, C. P.; Kalaria, R. N.; Sze, S. K. Degenerative Protein Modifications in the Aging Vasculature and Central Nervous System: A Problem Shared Is Not Always Halved. *Ageing Res. Rev.* **2019**, *53* (April), 100909. https://doi.org/10.1016/j.arr.2019.100909.

(18) Yuzhalin, A. E. Citrullination in Cancer. *Cancer Res.* **2019**, *79* (7), 1274–1284. https://doi.org/10.1158/0008-5472.CAN-18-2797.

(19) Fert-Bober, J.; Venkatraman, V.; Hunter, C. L.; Liu, R.; Crowgey, E. L.; Pandey, R.; Holewinski, R. J.; Stotland, A.; Berman, B. P.; Van Eyk, J. E. Mapping Citrullinated Sites in Multiple Organs of Mice Using Hypercitrullinated Library. *J. Proteome Res.* **2019**, *18* (5), 2270–2278. https://doi.org/10.1021/acs.jproteome.9b00118.

(20) Larsen, D. N.; Mikkelsen, C. E.; Kierkegaard, M.; Bereta, G. P.; Nowakowska, Z.; Kaczmarek, J. Z.; Potempa, J.; Højrup, P. Citrullinome of Porphyromonas Gingivalis Outer Membrane Vesicles: Confident Identification of Citrullinated Peptides. *Mol. Cell. Proteomics* **2020**, *19* (1), 167–180. https://doi.org/10.1074/mcp.RA119.001700.

(21) Hao, G.; Wang, D.; Gu, J.; Shen, Q.; Gross, S. S.; Wang, Y. Neutral Loss of Isocyanic Acid in Peptide CID Spectra: A Novel Diagnostic Marker for Mass Spectrometric Identification of Protein Citrullination. *J. Am. Soc. Mass Spectrom.* **2009**, *20* (4), 723–727. https://doi.org/10.1016/j.jasms.2008.12.012.

(22) Révész, Á.; Rokob, T. A.; Jeanne Dit Fouque, D.; Hüse, D.; Háda, V.; Turiák, L.; Memboeuf, A.; Vékey, K.; Drahos, L. Optimal Collision Energies and Bioinformatics Tools for Efficient Bottom-up Sequence Validation of Monoclonal Antibodies. *Anal. Chem.* **2019**, *91* (20), 13128–13135. https://doi.org/10.1021/acs.analchem.9b03362.

(23) Révész, Á.; Rokob, T. A.; Jeanne Dit Fouque, D.; Turiák, L.; Memboeuf, A.; Vékey, K.; Drahos, L. Selection of Collision Energies in Proteomics Mass Spectrometry Experiments for Best Peptide Identification: Study of Mascot Score Energy Dependence Reveals Double Optimum. *J. Proteome Res.* **2018**, *17* (5), 1898–1906. https://doi.org/10.1021/acs.jproteome.7b00912.

(24) Révész, Á.; Milley, M. G.; Nagy, K.; Szabó, D.; Kalló, G.; Csösz, É.; Vékey, K.; Drahos, L. Tailoring to Search Engines: Bottom-Up Proteomics with Collision Energies Optimized for Identification Confidence. *J. Proteome Res.* **2021**, *20* (1), 474–484. https://doi.org/10.1021/acs.jproteome.0c00518.

(25) Cao, L.; Tolić, N.; Qu, Y.; Meng, D.; Zhao, R.; Zhang, Q.; Moore, R. J.; Zink, E. M.; Lipton, M. S.; Paša-Tolić, L.; Wu, S. Characterization of Intact N- and O-Linked Glycopeptides Using Higher Energy Collisional Dissociation. *Anal. Biochem.* **2014**, *452* (1), 96–102. https://doi.org/10.1016/j.ab.2014.01.003.

(26) Riley, N. M.; Malaker, S. A.; Driessen, M. D.; Bertozzi, C. R. Optimal Dissociation Methods Differ for N- and O-Glycopeptides. *J. Proteome Res.* **2020**, *19* (8), 3286–3301. https://doi.org/10.1021/acs.jproteome.0c00218.

(27) Yang, H.; Yang, C.; Sun, T. Characterization of Glycopeptides Using a Stepped Higher-Energy C-Trap Dissociation Approach on a Hybrid Quadrupole Orbitrap. *Rapid Commun.*

Mass Spectrom. **2018**, *32* (16), 1353–1362. https://doi.org/10.1002/rcm.8191.

(28) Tabb, D. L.; Smith, L. L.; Breci, L. A.; Wysocki, V. H.; Lin, D.; Yates, J. R. Statistical Characterization of Ion Trap Tandem Mass Spectra from Doubly Charged Tryptic Peptides. *Anal. Chem.* **2003**, *75* (5), 1155–1163. https://doi.org/10.1021/ac026122m.

(29) Steckel, A.; Uray, K.; Turiák, L.; Gömöry, Á.; Drahos, L.; Hudecz, F.; Schlosser, G. Mapping the Tandem Mass Spectrometric Characteristics of Citrulline-Containing Peptides. *Rapid Commun. Mass Spectrom.* **2018**, *32* (11), 844–850. https://doi.org/10.1002/rcm.8105.

(30) Steckel, A.; Borbély, A.; Uray, K.; Schlosser, G. Quantification of the Effect of Citrulline and Homocitrulline Residues on the Collision-Induced Fragmentation of Peptides. *J. Am. Soc. Mass Spectrom.* **2020**, *31* (8), 1744–1750. https://doi.org/10.1021/jasms.0c00210.

(31) Steckel, A.; Uray, K.; Kalló, G.; Csosz, É.; Schlosser, G. Investigation of Neutral Losses and the Citrulline Effect for Modified H4 N-Terminal Pentapeptides. *J. Am. Soc. Mass Spectrom.* **2020**. https://doi.org/10.1021/jasms.9b00036.

(32) Lee, C. Y.; Wang, D.; Wilhelm, M.; Zolg, D. P.; Schmidt, T.; Schnatbaum, K.; Reimer, U.; Pontén, F.; Uhlén, M.; Hahne, H.; Kuster, B. Mining the Human Tissue Proteome for Protein Citrullination. *Mol. Cell. Proteomics* **2018**, *17* (7), 1378–1391. https://doi.org/10.1074/mcp.RA118.000696.

(33) Bern, M.; Kil, Y. J.; Becker, C. Byonic: Advanced Peptide and Protein Identification Software, Curr Protoc Bioinformatics. *Curr Protoc Bioinforma. Chapter 13* **2012**, Unit13. https://doi.org/10.1002/0471250953.bi1320s40.Byonic.

(34) Jin, Z.; Fu, Z.; Yang, J.; Troncosco, J.; Everett, A. D.; Eyk, J. E. Van. Identification and Characterization of Citrulline-Modified Brain Proteins by Combining HCD and CID Fragmentation. *Proteomics* **2013**, *13* (17), 2682–2691. https://doi.org/10.1002/pmic.201300064.Identification.

(35) Loos, T.; Opdenakker, G.; Van Damme, J.; Proost, P. Citrullination of CXCL8 Increases This Chemokine's Ability to Mobilize Neutrophils into the Blood Circulation. *Haematologica* **2009**, *94* (10), 1346–1353. https://doi.org/10.3324/haematol.2009.006973.

(36) Andrade, F.; Darrah, E.; Gucek, M.; Cole, R. N.; Rosen, A.; Zhu, X. Autocitrullination of Human Peptidyl Arginine Deiminase Type 4 Regulates Protein Citrullination during Cell Activation. *Arthritis Rheumatol.* **2010**, *62* (6), 1630–1640. https://doi.org/10.1002/art.27439.Autocitrullination.

(37) Pratesi, F.; Dioni, I.; Tommasi, C.; Alcaro, M. C.; Paolini, I.; Barbetti, F.; Boscaro, F.; Panza, F.; Puxeddu, I.; Rovero, P.; Migliorini, P. Antibodies from Patients with Rheumatoid Arthritis Target Citrullinated Histone 4 Contained in Neutrophils Extracellular Traps. *Ann. Rheum. Dis.* **2014**, *73* (7), 1414–1422. https://doi.org/10.1136/annrheumdis-2012-202765.

(38) Back to Basics: Optimize Your Search Parameters. http://www.matrixscience.com/blog/back-to-basics-optimize-your-search-parameters.html

(39) Steckel, A.; Schlosser, G. Citrulline Effect Is a Characteristic Feature of Deiminated Peptides in Tandem Mass Spectrometry. *J. Am. Soc. Mass Spectrom.* **2019**, *30* (9), 1586–1591. https://doi.org/10.1007/s13361-019-02271-x.

For Table of Contents Use Only

Successful identification of citrullinated peptides and the localization of citrullination sites depend on the collision energy. Energy-dependence of various features, including the Mascot and Byonic scores, as well as citrulline-specific fragmentation pathways were investigated, and optimal values are provided.